

Dual SDDP for risk-averse multistage stochastic programs

Bernardo Freitas Paulo da Costa,^{*} Vincent Leclère,[†]

April 21, 2023

Abstract

Risk-averse multistage stochastic programs appear in multiple areas and are challenging to solve. Stochastic Dual Dynamic Programming (SDDP) is a well-known tool to address such problems under time-independence assumptions. We show how to derive a dual formulation for these problems and apply an SDDP algorithm, leading to converging and deterministic upper bounds for risk-averse problems.

Keywords. Stochastic programming, Dynamic programming, SDDP, Risk measures, Duality

AMS subject classification. 90C15, 90C39, 49N15

1 Introduction

Multistage stochastic programming is a powerful framework with multiple applications [GZ13], *e.g.* in the finance, energy and supply chain sectors. If the uncertainty is finitely supported, those problems can be seen as large-scale deterministic problems. When there is more than 4 or 5 stages, the deterministic equivalent is usually too large to be solved directly. One of the most successful paradigms in this setting consists in leveraging time-independence assumptions to derive Bellman equations [Ber05]. The Stochastic Dual Dynamic Programming (SDDP) algorithm, and its numerous variants ([PP91, BDZ17, ZAS19, ACdC20]), consists in using those equations to derive approximations of the *cost-to-go* functions. It has been successfully used on a number of real-world problems, especially in the field of energy.

While the classical formulation of a multistage program is *risk-neutral*, meaning that we minimize an expected cost, a large part of the recent literature sparked by [Sha12, PdMF13, STdCS13] has been devoted to efficiently introduce *risk aversion* in this framework, in particular inside the SDDP algorithm. Coherent risk measures [ADEH99] have become a usual tool to represent risk aversion in stochastic optimization problems. In multistage stochastic programming, minimizing a risk measure of the sum of costs leads to time-inconsistency. The easiest way to come up with a time-consistent risk-averse problem is to use composed Markovian risk measures [Rus10], which, roughly speaking, means replacing the expectation by a risk measure inside the dynamic programming equation.

More precisely, let $(\Omega, \mathcal{F}, \mathbb{P})$ be a probability space, and $\{\omega_t\}_{t \in [T]}$ be a sequence of finitely supported, independent random variables (by convention, boldscript refers to random variables,

^{*}EMAp-FGV, Rio de Janeiro, Brazil

[†]CERMICS, École des Ponts, Marne-la-Vallée, France

normal script to an element of their support, and equalities between random variables hold almost surely.) We consider the following risk-averse multistage linear program (RA-MSLP)

$$\min_{\mathbf{x}_t, \mathbf{y}_t} \rho_1 \left(\mathbf{c}_1^\top \mathbf{y}_1 + \rho_{2|\omega_1} \left(\cdots + \rho_{T|\omega_{[T-1]}} (\mathbf{c}_T^\top \mathbf{y}_T) \right) \right) \quad (1a)$$

$$\text{s.t. } \mathbf{A}_t \mathbf{x}_t + \mathbf{B}_t \mathbf{x}_{t-1} + \mathbf{T}_t \mathbf{y}_t = \mathbf{d}_t \quad \forall t \in [T] \quad (1b)$$

$$0 \leq \mathbf{x}_t \leq \bar{\mathbf{x}}_t, \quad 0 \leq \mathbf{y}_t \leq \bar{\mathbf{y}}_t \quad \forall t \in [T] \quad (1c)$$

$$\mathbf{x}_t, \mathbf{y}_t \preceq \boldsymbol{\omega}_{[t]} \quad \forall t \in [T] \quad (1d)$$

where $\rho_{t|\omega_{[t]}}$ is a coherent risk measure conditional on the past noises $\boldsymbol{\omega}_{[t]} := \{\boldsymbol{\omega}_1, \dots, \boldsymbol{\omega}_t\}$, all equalities hold almost surely, and constraint (1d) is the *non-anticipativity* constraint, stating that decisions $\mathbf{x}_t, \mathbf{y}_t$ are measurable with respect to $\boldsymbol{\omega}_{[t]} := \{\boldsymbol{\omega}_1, \dots, \boldsymbol{\omega}_t\}$. Convexity of ρ_t is crucial both for the SDDP algorithm and the duality theory developed here. Moreover, in this paper we restrict ourselves to polyhedral risk measures (defined in Section 2.2) to avoid dealing with technical constraint qualification considerations which would distract the reader. Finally, note that, by construction, the nested multistage risk measure used in Problem (1) is time-consistent.

Since $\{\boldsymbol{\omega}_t\}_{t \in [T]}$ is a sequence of *independent* random variables, Dynamic Programming leads to the following recursion:

$$V_{T+1}(\mathbf{x}_T) = 0, \quad (2)$$

$$\begin{aligned} V_t(\mathbf{x}) = \min_{\mathbf{x}_t, \mathbf{y}_t} \quad & \rho_t [\mathbf{c}_t^\top \mathbf{y}_t + V_{t+1}(\mathbf{x}_t)] \\ \text{s.t.} \quad & \mathbf{A}_t \mathbf{x}_t + \mathbf{B}_t \mathbf{x} + \mathbf{T}_t \mathbf{y}_t = \mathbf{d}_t \\ & 0 \leq \mathbf{x}_t \leq \bar{\mathbf{x}}_t, \quad 0 \leq \mathbf{y}_t \leq \bar{\mathbf{y}}_t \end{aligned} \quad (3)$$

where the value of Problem (1) is given by $V_1(\mathbf{x}_0)$.

The classical SDDP algorithm builds outer approximations of the cost-to-go functions V_t , leading to exact lower bounds on the problem. In a risk-neutral framework, upper bounds can be estimated via Monte Carlo sampling. Unfortunately, it is unclear how to extend such statistical methods to the risk-averse setting [STdCS13]. Instead of statistical upper bounds, one can use exact upper bounds: Through backward recursion ([PdMF13]); by maintaining upper and lower bounds for all value functions ([BDZ17, DDB20]); or using Fenchel duality ([LCC⁺20, GSC19]). Up to now, the first approach has not been used to compute improving upper bounds along SDDP iterations, while the second approach relies on a *problem-child* node selection method. Finally, the last approach was developed only in a risk-neutral setting. The aim of this work is to adapt the latter approach to a risk-averse setting. By dualizing the extensive formulation of the risk-averse MLSP problem, and recognizing a time-decomposition, we obtain a Bellman recursion on which SDDP can be applied, yielding converging exact upper bounds.

Contributions In this paper we i) derive a dual formulation of RA-MLSP with polyhedral risk measure; ii) show that it is time-decomposable and solvable through SDDP, yielding exact upper bounds of the original problem; iii) link the value function of the dual formulation with the co-perspective of the primal value function; and iv) illustrate the approach with numerical results.

2 Time decomposition of the dual of a risk averse MSLP

2.1 Risk-averse duals with AV@R

We start by showing how to build the dual problem in a very specific setting: for a single step of the recursion, with no upper bounds on \mathbf{x}_t and \mathbf{y}_t , and when the risk measure ρ is a convex combination of the mean and the α -AV@R, given by, for $\alpha \in (0, 1)$ and $\beta \in [0, 1]$,

$$\rho[\boldsymbol{\theta}] := \beta \mathbb{E}[\boldsymbol{\theta}] + (1 - \beta) \text{AV@R}_\alpha[\boldsymbol{\theta}]. \quad (4)$$

This risk measure assumes an underlying probability for the scenarios, with respect to which one calculates the expectation and the AV@R. The risk measures we employ in the example in section 4.2 will be of this class.

We rewrite equation (3) using the Rockafellar-Uryasev representation of AV@R, with $\boldsymbol{\theta}$ as epigraphical variables for the scenario costs. For simplicity, we represent a random variable as a vector in \mathbb{R}^J , denoted with bold letters such as $\mathbf{x} = (x_1, \dots, x_J)$, and the expectation $\mathbb{E}[\mathbf{x}]$ is the sum $\sum p_j x_j$. So, the value of $V_t(x_{t-1})$ is given by:

$$\begin{aligned} \inf_{\mathbf{x}, \mathbf{y}; q, \boldsymbol{\theta}, \mathbf{u}} \quad & \beta \mathbb{E}[\boldsymbol{\theta}] + (1 - \beta) [q + \frac{1}{\alpha} \mathbb{E}[\mathbf{u}]] \\ \text{s.t.} \quad & q + u_j \geq \theta_j \quad \forall j \in [J] \\ & \theta_j \geq \mathbf{c}_j^\top \mathbf{y}_j + V_t(x_j) \quad \forall j \in [J] \\ & A_j x_j + B_j x_{t-1} + T_j y_j = d_j \quad \forall j \in [J] \\ & x_j, y_j, u_j \geq 0 \quad \forall j \in [J] \end{aligned} \quad (5)$$

We define dual multipliers for every constraint: in order, $\boldsymbol{\delta}$, $\boldsymbol{\gamma}$, $\boldsymbol{\lambda}$, $\boldsymbol{\mu}$, $\boldsymbol{\nu}$, and $\boldsymbol{\eta}$. With the expectation inner product, this yields the Lagrangian:

$$\begin{aligned} (1 - \beta)q + \beta \mathbb{E}[\boldsymbol{\theta}] + (1 - \beta)/\alpha \cdot \mathbb{E}[\mathbf{u}] + \mathbb{E}[\boldsymbol{\gamma}(\mathbf{c}^\top \mathbf{y} + V(\mathbf{x}) - \boldsymbol{\theta}) + \boldsymbol{\delta}(\boldsymbol{\theta} - q - \mathbf{u})] \\ + \mathbb{E}[\boldsymbol{\lambda}^\top (\mathbf{A}\mathbf{x} + \mathbf{B}x_{t-1} + \mathbf{T}\mathbf{y} - \mathbf{d})] - \mathbb{E}[\boldsymbol{\mu}^\top \mathbf{x} + \boldsymbol{\nu}^\top \mathbf{y} + \boldsymbol{\eta}\mathbf{u}] \end{aligned}$$

Eliminating the multipliers $\boldsymbol{\nu}$ and $\boldsymbol{\eta}$, we obtain the dual problem

$$\begin{aligned} \sup_{\boldsymbol{\lambda}, \boldsymbol{\gamma}, \boldsymbol{\delta}, \boldsymbol{\mu}} \quad & \mathbb{E} \left[\boldsymbol{\lambda}^\top (\mathbf{B}x_{t-1} - \mathbf{d}) + \inf_{\mathbf{x}} \left[(\mathbf{A}^\top \boldsymbol{\lambda} - \boldsymbol{\mu})^\top \mathbf{x} + \gamma V_t(\mathbf{x}) \right] \right] \\ \text{s.t.} \quad & \mathbb{E}[\boldsymbol{\delta}] = (1 - \beta) \\ & 0 \leq \delta_j \leq \frac{1 - \beta}{\alpha} \quad \forall j \in [J] \\ & \gamma_j = \beta + \delta_j \quad \forall j \in [J] \\ & \gamma_j \mathbf{c}_j + T_j^\top \boldsymbol{\lambda}_j \geq 0 \quad \forall j \in [J] \\ & \mu_j \geq 0 \quad \forall j \in [J] \end{aligned} \quad (6)$$

Observe that the variable γ represents the “change-of-measure” implied by the mean-AV@R combination [SDR09]. Indeed, γ is at least $\beta \leq 1$, and some events will have an increased contribution, up to $\frac{1 - \beta}{\alpha}$, so that $\mathbb{E}[\gamma] = 1$.

2.2 Polyhedral risk measures and duality

To extend the previous approach to more general risk measures, we adopt a distributionally robust point of view. We consider a *polyhedral risk measure* ρ , that is, a coherent risk measure of the form

$$\rho : \mathbf{t} \mapsto \sup_{\mathbb{Q} \in \mathcal{Q}} \mathbb{E}_{\mathbb{Q}}[\mathbf{t}] = \max_{k \in [K]} \{\mathbb{E}_{\mathbb{Q}^k}[\mathbf{t}]\}, \quad (7)$$

where $\mathcal{Q} = \text{conv}(\{\mathbb{Q}^k\}_{k \in [K]})$. Polyhedral risk measures can be either chosen as interpretable risk-measures (e.g. AV@R in a finite setting) or as the worst case among a set of probabilities estimated by various experts. Since we don't assume a reference probability, we resort to describing the extremal risk measures, which may be very numerous. This also changes the interpretation of the dual variables γ : now they correspond to supporting probabilities, instead of a change-of-measure.

We denote the elements of the support of ω by $\omega_1, \dots, \omega_J$, and let $q_j^k := \mathbb{Q}^k[\omega = \omega_j]$. Now, $V_t(x_{t-1})$ is given by:

$$\begin{aligned} \inf_{\mathbf{x}, \mathbf{y}; z, \boldsymbol{\theta}} \quad & z & (8) \\ \text{s.t.} \quad & z \geq \sum_{j \in [J]} q_j^k \theta_j & \forall k \quad [\phi_k] \\ & \theta_j \geq c_j^\top y_j + V_{t+1}(x_j) & \forall j \quad [\gamma_j] \\ & A_j x_j + B_j x_{t-1} + T_j y_j = d_j & \forall j \quad [\lambda_j] \\ & 0 \leq x_j \leq \bar{x}_t & \forall j \quad [\mu_j, \zeta_j] \\ & 0 \leq y_j \leq \bar{y}_t & \forall j \quad [\nu_j, \xi_j] \end{aligned}$$

Proceeding analogously to the AV@R case above, we introduce dual multipliers as indicated in the brackets, and obtain the following dual problem

$$\begin{aligned} \sup_{\substack{\phi_k, \gamma_j, \lambda_j, \\ \mu_j, \zeta_j, \xi_j}} \quad & \sum_{j \in [J]} \left[\lambda_j^\top (B_j x_{t-1} - d_j) - \bar{x}_t \zeta_j - \bar{y}_t \xi_j \right. \\ & \left. + \inf_{x_j} (A_j^\top \lambda_j - \mu_j + \zeta_j)^\top x_j + \gamma_j V_{t+1}(x_j) \right] & (9) \\ \text{s.t.} \quad & \sum_k \phi_k = 1, \quad \phi_k \geq 0, \\ & \sum_k \phi_k q_j^k = \gamma_j \geq 0 & \forall j \\ & \gamma_j c_j + T_j^\top \lambda_j + \xi_j \geq 0 & \forall j \\ & \mu_j, \zeta_j, \xi_j \geq 0 & \forall j. \end{aligned}$$

The constraints on ϕ_k are equivalent to describing the vector of γ_j 's as a convex combination of the extreme probabilities \mathbb{Q}^k . Therefore, one can rewrite problem (9) to include the constraint $\{\gamma_j\}_{j \in [J]} \in \mathcal{Q}$ instead of the first two lines. This shows that the variables γ_j correspond to one supporting probability of the risk measure ρ . In particular, if a given scenario is *effective*, in the sense of [RBHdM19], then there exists an optimal γ which charges this scenario.

Moreover, the last two constraints here correspond exactly to the last two in problem (6), which emphasizes the similarity between (9) and (6).

2.3 Multistage risk averse problem duality

We now extend the duality to the full multistage problem. In the stagewise independent setting, we let Ω_t be the set of all possible realizations of ω_t , and the risk measure ρ_t is defined by $\rho_t = \sup_{\mathbb{Q} \in \mathcal{Q}_t} \mathbb{E}_{\mathbb{Q}}[\cdot]$, for a polyhedral subset \mathcal{Q}_t of probability measures on Ω_t . The tree \mathcal{T} describing the stochastic process is such that each node n of depth t is associated with a possible

value of $\omega_{[t]} = (\omega_1, \dots, \omega_t)$. For any node n , the set of its children is denoted by C_n , and \mathcal{L} is the set of leaves of \mathcal{T} .

In the spirit of the previous section, we introduce variables z_n to stand for the risk-adjusted value of our problem starting from node n , and θ_m represents the cost-to-go following the branch of node $m \in C_n$. To reduce notational burden, we assume that, for all t , $\rho_t = \rho$. Then, the risk averse problem (1), with value $V_{n_0}(\tilde{x}_{n_0})$, can be written as the following linear program:

$$\begin{aligned}
\min \quad & z_0 \\
\text{s.t.} \quad & \sum_{m \in C_n} q_m^k \theta_m \leq z_n & \forall n, \forall k \in [K] & [\Phi_n^k] \\
& c_m^\top y_m + z_m \leq \theta_m & \forall m \in \mathcal{T} \setminus \{n_0\} & [\gamma_m] \\
& A_m x_m + B_m \tilde{x}_n + T_m y_m = d_m & \forall n, \forall m \in C_n & [\lambda_m] \\
& z_\ell = 0 & \forall \ell \in \mathcal{L} & [\eta_\ell] \\
& x_m = \tilde{x}_m & \forall m \in \mathcal{T} \setminus \{n_0\} & [\pi_m] \\
& 0 \leq \tilde{x}_m \leq \bar{x}_m & \forall m \in \mathcal{T} \setminus \{n_0\} & [\mu_m, \zeta_m] \\
& 0 \leq y_m \leq \bar{y}_m & \forall m \in \mathcal{T} \setminus \{n_0\} & [\mu_m, \xi_m]
\end{aligned} \tag{10}$$

where, when unspecified, $\forall n$ stands for $\forall n \in \mathcal{T} \setminus \mathcal{L}$, \tilde{x}_{n_0} is a parameter and not a variable, and we add the equalities $x_m = \tilde{x}_m$ to highlight the time dynamics.

Defining $\gamma_{n_0} = 1$, the linear programming dual of problem (10) is

$$\begin{aligned}
\sup_{\Phi, \gamma, \pi, \lambda} \quad & \pi_{n_0}^\top \tilde{x}_{n_0} - \sum_m \lambda_m^\top d_m + \bar{x}_m^\top \zeta_m + \bar{y}_m^\top \xi_m \\
\text{s.t.} \quad & \sum_{k \in [K]} \Phi_n^k = \gamma_n & \forall n & [z_n] \\
& \sum_{k \in [K]} \Phi_n^k q_m^k = \gamma_m \geq 0 & \forall n, \forall m \in C_n & [\theta_m] \\
& \pi_{n_0} = \sum_{m \in C_{n_0}} B_m^\top \lambda_m \\
& \pi_n \leq \zeta_n + \sum_{m \in C_n} B_m^\top \lambda_m & \forall n \in \mathcal{T} \setminus \{n_0\} & [\tilde{x}_m] \\
& \pi_m + A_m^\top \lambda_m = 0 & \forall m & [x_m] \\
& \gamma_m c_m + T_m^\top \lambda_m + \xi_m \geq 0 & \forall m & [y_m] \\
& \Phi_n^k \geq 0 & \forall n, \forall k \in [K] \\
& \zeta_m \geq 0, \xi_m \geq 0 & \forall m
\end{aligned}$$

where we keep $\forall n$ to imply $n \in \mathcal{T} \setminus \mathcal{L}$ as above, and unspecified $\forall m$, \sum_m range over $m \in \mathcal{T} \setminus \{n_0\}$.

Note that Φ_n^k can be seen as barycentric coordinates of the extreme points of \mathcal{Q} . Thus, the first two constraints can be more compactly written as $(\gamma_m)_{m \in C_n} \in \gamma_n \mathcal{Q}$.

By backward recursion, this problem can be solved through the following recursive equations, where, for all leaves $\ell \in \mathcal{L}$, $D_\ell(\pi_\ell, \gamma_\ell) = -\bar{x}_\ell^\top \max\{\pi_\ell, 0\}$, and for all nodes $n \in \mathcal{T} \setminus \mathcal{L}$, $D_n(\pi_n, \gamma_n)$

is given as the value of

$$\begin{aligned}
& \sup_{\substack{\pi_m, \gamma_m, \lambda_m \\ \zeta_n, \xi_m \geq 0}} \mathbb{1}_{\{n=n_0\}} \pi_{n_0}^\top \tilde{x}_{n_0} - \tilde{x}_n^\top \zeta_n + \\
& \quad \sum_{m \in C_n} -\lambda_m^\top d_m - \bar{y}_m^\top \xi_m + D_m(\pi_m, \gamma_m) \\
& \text{s.t.} \quad (\gamma_m)_{m \in C_n} \in \gamma_n \mathcal{Q} \\
& \quad \zeta_n + \sum_{m \in C_n} B_m^\top \lambda_m \geq \pi_n \\
& \quad \pi_m + A_m^\top \lambda_m = 0, \quad \forall m \in C_n \\
& \quad \gamma_m c_m + T_m^\top \lambda_m + \xi_m \geq 0, \quad \forall m \in C_n
\end{aligned} \tag{11}$$

By the independence assumption, a backward induction shows that $D_n = D_{n'}$ for all nodes n and n' of the same depth. Thus, defining $D_T(\pi_T, \gamma_T) = -\tilde{x}_T^\top \max\{\pi_T, 0\}$, we obtain the following recursion for the dual value functions:

$$\begin{aligned}
D_t(\pi_t, \gamma_t) = & \sup_{\substack{\zeta, \gamma_j, \\ \lambda_j, \pi_j, \xi_j}} -\tilde{x}_t^\top \zeta + \sum_{j \in [J_t]} \left[-d_j^\top \lambda_j - \bar{y}_{t+1}^\top \xi_j + D_{t+1}(\pi_j, \gamma_j) \right] \\
& \text{s.t.} \quad (\gamma_j)_{j \in [J_t]} \in \gamma_t \mathcal{Q} \\
& \quad \zeta + \sum_{j \in [J_t]} B_j^\top \lambda_j \geq \pi_t \\
& \quad \pi_j + A_j^\top \lambda_j = 0 \quad \forall j \in [J_t] \\
& \quad \gamma_j c_j + T_j^\top \lambda_j + \xi_j \geq 0 \quad \forall j \in [J_t] \\
& \quad \xi_j \geq 0, \quad \zeta \geq 0
\end{aligned} \tag{12}$$

This decomposition satisfies the RCR conditions. Indeed, for every π_t and every $\gamma_t \geq 0$, any $\gamma \in \gamma_t \mathcal{Q}$ and $\lambda = 0$ are admissible, using slack variable ζ as needed. Then, π_j are given by the $\pi_j + A_j^\top \lambda_j = 0$, and the remaining constraints can be adjusted using ξ_j .

Remark 1. Relatively complete recourse in a dual formulation is not guaranteed (see for example [GSC19]). In our setting, the explicit upper bounds of (1c) ensure RCR. The existence of such upper bounds is equivalent to the existence of exact penalization coefficients in the dual, which is the tool used in [GSC19] to deal with this difficulty. Alternatively, we could incorporate feasibility cuts in the algorithm.

2.4 Bounding the dual state

With our boundedness assumption, we have relatively complete recourse in the dual. To prove convergence, we still need to ensure that the dual state remains bounded.

By assumption, we know that there exists an optimal primal solution. Further, by linear programming duality, we know that there exists an optimal dual solution. The marginal interpretation of the Lagrange multiplier π (see Problem (10)) states that, for each node, the optimal dual π_n is a subgradient of the primal value function for $\gamma_n = 1$. In particular, π_n/γ_n can be bounded by the Lipschitz constant of the primal value function V_n . In the independent setting, assuming that V_t is L_t -Lipschitz continuous on its domain, we can add the constraint

$|\pi_j| \leq \gamma_j L_{t+1}$ to (12) for each j , without changing its value. This method is similar to the compactification process through Lipschitz-regularization used in [LCC⁺20].

Therefore, we use the compactified recursion presented in (13). Since it has RCR and bounded states, the SDDP algorithm on this recursion converges. This is illustrated in section 4.

$$D_t(\pi_t, \gamma_t) = \sup_{\substack{\zeta, \gamma_j, \lambda_j, \pi_j, \xi_j \\ \text{s.t.}}} -\bar{x}_t^\top \zeta + \sum_{j \in [J]} -d_j^\top \lambda_j - \bar{y}_{t+1}^\top \xi_j + D_{t+1}(\pi_j, \gamma_j) \quad (13)$$

$$\begin{aligned} & \gamma \in \gamma_t \mathcal{Q} \\ & \zeta + \sum_j B_j^\top \lambda_j \geq \pi_t \\ & \pi_j + A_j^\top \lambda_j = 0 & \forall j \in [J_t] \\ & \gamma_j c_j + T_j^\top \lambda_j + \xi_j \geq 0 & \forall j \in [J_t] \\ & |\pi_j| \leq \gamma_j L_{t+1} & \forall j \in [J_t] \\ & \zeta \geq 0, \xi_j \geq 0 \end{aligned}$$

3 Dual risk averse Bellman operator

We introduce convex analysis tools that shed new light on the link between the primal and dual value functions given in Section 2.

3.1 Homogeneous Fenchel duality

Let $f : \mathbb{R}^n \rightarrow (-\infty, \infty]$ be a proper lower semicontinuous convex function. Recall (see [Com18] for more details) that the *perspective function* of f , denoted \tilde{f} , is a convex, lower-semicontinuous function of \mathbb{R}^{n+1} , such that $\tilde{f}(x, \gamma) = \gamma f(x/\gamma)$ for any positive number γ .

Recall that the Fenchel conjugate of f is

$$f^* : \mathbb{R}^n \rightarrow \overline{\mathbb{R}} : \psi \mapsto \sup_{x \in \mathbb{R}^n} \psi^\top x - f(x). \quad (14)$$

Inspired by the recurrences in (6) and (9), we introduce the *coperspective function*:

Definition 2. Let $f : \mathbb{R}^n \rightarrow \overline{\mathbb{R}}$. The coperspective of f is the perspective of the Fenchel conjugate, that is $(f^*)^\sim$, that we denote f^\boxtimes . In particular, for $\psi \in \mathbb{R}^n$ and $\gamma \in \mathbb{R}_{++}$, we have

$$f^\boxtimes(\psi, \gamma) := \sup_{x \in \mathbb{R}^n} \psi^\top x - \gamma f(x). \quad (15)$$

Remark 3. The coperspective is jointly convex in (ψ, γ) , lower semicontinuous, and a positively homogeneous function of degree 1: for all $t > 0$,

$$f^\boxtimes(t \cdot \psi, t \cdot \gamma) = t \cdot f^\boxtimes(\psi, \gamma).$$

Remark 4. Cuts for a convex function and its perspective are essentially equivalent. If $f(x) \geq f(x_0) + g^\top(x - x_0) = \theta + g^\top x$, then

$$\begin{aligned} \tilde{f}(x, \gamma) &= \gamma \cdot f(x/\gamma) \geq \gamma f(x_0) + \gamma g^\top(x/\gamma - x_0) \\ &\geq \gamma f(x_0) + g^\top(x - \gamma \cdot x_0) \\ &\geq \theta \cdot \gamma + g^\top x \end{aligned}$$

Similarly, if $\tilde{f}(x, \gamma) \geq \theta \cdot \gamma + g^\top x + \beta$, then $f(x) \geq g^\top x + \theta + \beta$. Note that if the cut for \tilde{f} is exact we can assume $\beta = 0$.

3.2 Duality and conjugate value functions

Consider a polyhedral risk measure ρ and the associated risk-averse Bellman operator \mathcal{B} that, to any cost-to-go function V and initial state x_{t-1} associates the value of Problem (8).

The coperspective of $\mathcal{B}(V)$ can be calculated using (9). Leveraging positive homogeneity, for $\psi_0 \in \mathbb{R}^n$ and $\gamma_0 > 0$, we get that $\mathcal{B}(V)^\boxtimes(\psi_0, \gamma_0)$ is given by

$$\begin{aligned} & \sup_{x_0} \psi_0^\top x_0 \\ & + \inf_{\substack{\gamma, \lambda, \mu \\ \zeta, \xi}} \sum_{j \in [J]} \lambda_j^\top (d_j - B_j x_0) + \xi_j^\top \bar{y}_{t+1} + \zeta_j^\top \bar{x}_{t+1} + V^\boxtimes(\mu_j - A_j^\top \lambda_j - \zeta_j, \gamma_j) \\ & \text{s.t. } \gamma \in \gamma_0 \mathcal{Q} \\ & \quad \gamma_j c_j + \xi_j + T_j^\top \lambda_j \geq 0 \quad \forall j \\ & \quad \mu_j, \zeta_j, \xi_j \geq 0 \quad \forall j. \end{aligned} \tag{16}$$

Note that, if V is polyhedral, so are its Fenchel dual and its perspective. Thus, by linear programming duality, we can interchange sup and inf to obtain

$$\begin{aligned} [\mathcal{B}(V)]^\boxtimes(\psi_0, \gamma_0) = & \inf_{\substack{\gamma, \lambda \\ \mu, \zeta, \xi}} \sum_{j \in [J]} \lambda_j^\top d_j + \xi_j^\top \bar{y}_{t+1} + \zeta_j^\top \bar{x}_{t+1} + V^\boxtimes(\psi_j, \gamma_j) \\ & \text{s.t. } \sum_j B_j^\top \lambda_j = \psi_0 \\ & \quad \gamma \in \gamma_0 \mathcal{Q} \\ & \quad \gamma_j c_j + \xi_j + T_j^\top \lambda_j \geq 0 \quad \forall j \\ & \quad \psi_j = \mu_j - A_j^\top \lambda_j - \zeta_j \quad \forall j. \end{aligned} \tag{17}$$

This equation defines a risk-neutral LBO \mathcal{B}^\boxtimes that takes a *homogeneous* recourse function V^\boxtimes and returns another homogeneous convex function of the same dimension. We call this operator the *projective dual Bellman operator* associated to \mathcal{B} .

Comparing (12) and (17), we notice the decomposition is not done at the same time-step for all variables: in the first one, ζ is a single variable, relaxing the incoming dual state constraint; whereas in the second, it relaxes the outgoing dual state constraint. Substituting $\pi_j = \psi_j + \zeta_j - \mu_j$, we obtain the following proposition, linking the coperspectives of the primal value functions with the value functions of the dual problem.

Proposition 5. *For $t \in [T]$, if the dual value function D_t is defined by (12), and V_t is the primal value function defined by (3) then*

$$D_t(\pi_t, \gamma_t) = - \inf_{\substack{\zeta_t + \psi_t \geq \pi_t \\ \zeta_t \geq 0}} \bar{x}_t^\top \zeta_t + V_t^\boxtimes(\psi_t, \gamma_t).$$

In particular, D_t is a concave, positively homogeneous, one-sided Lipschitz regularization of V_t^\boxtimes .

Further, the value of primal Problem (1) is $\sup_{\pi_0} \pi_0^\top x_0 + D_0(\pi_0, 1)$.

This proposition paves the way to a dual SDDP algorithm. Indeed, it was shown in [LCC⁺20] that SDDP can be applied to any sequence of functions linked through linear Bellman operators (LBO) like \mathcal{B}^\boxtimes .

4 Examples

In this section, we provide an algorithm, in the lineage of SDDP, for the risk-averse dual problem given by the recursion (13). Then, we close with one numerical example from a real-world

problem. A more comprehensive discussion on the algorithm, including implementation details, can be found in the appendix. There, one will also find further results on the application of our algorithm.

4.1 A dual risk-averse algorithm

The recursion of (perspective) value functions D_t given by (13) can be solved by recursively constructing piecewise linear (upper) approximations, which we call \mathfrak{D}_t . As usual, one needs to ensure that the domain of the state variables π_t and γ_t remains bounded. Since all γ_t remain in $[0, 1]$, we only need bounds for π_t , which we assume are given by the user as the Lipschitz constants L_t for the primal value functions V_t . In our experiments, the Lipschitz constant estimation was not critical: Increasing L_t by a factor 10 or 100 had a negligible impact after 50 iterations, as can be seen in section C of the companion. Moreover, one needs a starting upper bound for \mathfrak{D}_t . These can be obtained, for example, choosing $\pi_t = 0$ and $\gamma_t = 1$, and constructing cuts from $t = T - 1$ back to $t = t_0$.

The first stage problem, corresponding to $t = t_0$, is slightly different. It is obtained as the fusion of the “zero-th stage” containing π_{n_0} as a decision variable, and the first stage in (13). Furthermore, since x_{n_0} is fixed, there’s no corresponding slack variables μ_{n_0} and ζ_{n_0} , so it must satisfy

$$\sum_{j \in [J_0]} B_j^\top \lambda_j = \pi_0. \quad (18)$$

With this, we can now present how one can perform Bellman iterations on the recursion defined by (13) to obtain convergence. We highlight the following differences with the primal SDDP:

- Computing $D_t(\pi, \gamma)$ cannot be decomposed by realization of ω_t due to the coupling constraint $\zeta + \sum_{j \in [J_t]} B_j^\top \lambda_j \geq \pi_t$. In particular, the forward pass is as demanding as the backward pass, and yields cuts. Furthermore, we have one next-state variable per possible realization of ω_t , which means that, when adding a single cut to the approximation of D_{t+1} , we are adding J_t constraints.
- In the forward step, we choose the realization j according to a (smoothed) “importance sampling” procedure, with weight $\gamma_j + \varepsilon$.
- By homogeneity, we normalize the state variables (π_j, γ_j) that will be used in the next step of the forward pass to have $\gamma_{t+1} = 1$, unless we are in a branch where $\gamma_t = 0$. This has had a positive impact in the numerical stability of the algorithm.
- Finally, by remark 4, we ensure that, for every cut, its parameter β is always zero.

Naturally, one can couple this algorithm with (say) SDDP running on the primal. This keeps track of both upper and lower bounds, therefore allowing to stop based on a prescribed *tolerance*, instead of just a maximum number of iterations as described above.

Let us close this section with two remarks. First, even if this algorithm uses only forward passes, one could use backward passes for computing cuts, as in the classical SDDP algorithm. This would require solving approximately twice the number of optimization problems, but would include in the backward pass the updated value function, which could potentially speed up the convergence of the algorithm. Furthermore, this algorithm is easily amenable to standard cut-selection techniques, which can be useful to reduce the computational burden of each iteration.

Algorithm 1: Dual Risk-Averse SDDP

Data: upper bounds $\mathfrak{D}_t^0 \geq D_t$ and bounds L_t for $|\pi_t|$

Result: upper bound on the value of (13)

```
1 for  $k = 0$  to  $N$  do
2   Solve the first stage problem to obtain  $\pi_0$ , and set  $\gamma_0 = 1$ 
3   if  $k == N$  then Return upper bound
4
5   for  $t = 0$  to  $T - 1$  do                                     // forward pass
6     Solve problem (13) with  $\mathfrak{D}_{t+1}^k$  instead of  $D_{t+1}$ 
7     Compute a cut for  $D_t$  using the optimal multipliers for  $\pi_t$  and  $\gamma_t$ 
8     Choose a branch  $\hat{j}$  according to probabilities  $\gamma_j + \varepsilon$ 
9     if  $\gamma_{\hat{j}} > 0$  then
10      Set  $\pi_{t+1} \leftarrow \pi_{\hat{j}} / \gamma_{\hat{j}}$ , and  $\gamma_{t+1} \leftarrow 1$ 
11    else
12      Set  $\pi_{t+1} \leftarrow \pi_{\hat{j}}$ , and  $\gamma_{t+1} \leftarrow 0$ 
```

4.2 Numerical experiments

We present here a numerical example. Further details and other results are given in the companion, and the implementation in julia, along with other examples, can be found at <https://github.com/bfpc/DualSDDP.jl>.

This example comes from the Brazilian Hydrothermal Energy planning problem, where the reservoirs and hydro dams are aggregated into 4 subsystems, and there is a 5th node in the network, as an interconnection. Therefore, it contains 4 state variables (the stored energy in each reservoir), 9 equality constraints for the dynamics (4 for the states, and 5 for demand in each node), and a total of 164 control variables, accounting for hydro and thermal energy produced, and energy exchange among the nodes in the system. The uncertainty at each time step is the inflow for each aggregated reservoir, and is different for each time step, corresponding to different months of the year.

For this example, we take 12 stages and 82 inflow realizations per stage (thus 82^{12} scenarios). We have natural bounds for every state variable, given by the reservoirs' limits, and control variables (power output, line capacities, ...). The risk measure considered was a combination of expectation and AV@R, given by $\beta\mathbb{E} + (1 - \beta)\text{AV@R}_\alpha$. In this problem, the highest marginal cost is given by load shedding, which yields estimates for the Lipschitz constants we use.

In Figure 1, we present the evolution of the bounds obtained by the primal SDDP, our dual SDDP algorithm, as well the one shot backward bounds of [PdMF13] (Philpott UB), computed every 50 iterations based on the trajectories from primal SDDP, and the upper and lower bounds provided by the problem-child method of [BDZ17] (Baucke UB / LB). This is done for various level of risk aversion. Note that, on this problem, the dual upper bound always outperform the problem-child method. It also slightly beat the primal one-shot upper bound in the most risk-averse case. This is also observed on the other numerical experiments available at <https://github.com/bfpc/DualSDDP.jl>.

Finally, we noticed that each iteration of the dual is between 30 and 15 times slower than primal iteration, being larger for higher branching sizes.

# branches	P-SDDP	D-SDDP	Problem Child
10	0.023	0.166	0.109
20	0.054	0.523	0.224
40	0.113	2.366	0.402
80	0.274	5.739	0.813

Table 1: Single iteration time in sec (around $it = 100$)

This is expected, since each problem in the dual formulation includes all inflow realizations and a linking constraint among all of them, whereas the primal problem also allows decomposing each time step in separate problems for each branch.

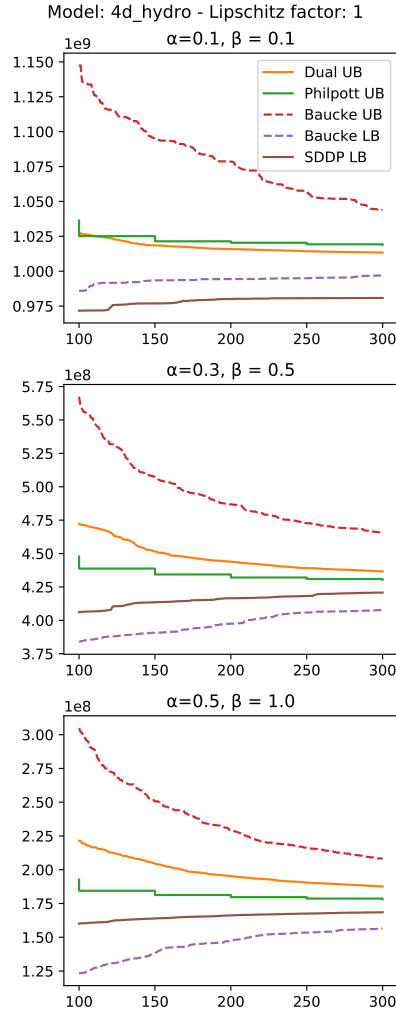


Figure 1: Bounds evolution for hydrothermal problem.

Acknowledgements We would like to thank the editor and an anonymous referee for their suggestions which improved the presentation of our results. We also thank Lucas Merabet for

his comments.

The first author is partly supported by project COPPETEC-23145. The second author benefited from the support of FMJH-PGMO and from EDF.

References

- [ACdC20] Shabbir Ahmed, Filipe Goulart Cabral, and Bernardo Freitas Paulo da Costa. Stochastic lipschitz dynamic programming. *Mathematical Programming*, pages 1–39, 2020.
- [ADEH99] Philippe Artzner, Freddy Delbaen, Jean-Marc Eber, and David Heath. Coherent measures of risk. *Mathematical finance*, 9(3):203–228, 1999.
- [BDZ17] Regan Baucke, Anthony Downward, and Golbon Zakeri. A deterministic algorithm for solving multistage stochastic programming problems. *Optimization On-line*, 2017.
- [Ber05] Dimitri P Bertsekas. *Dynamic programming and optimal control*, volume 1 & 2. Athena Scientific Belmont, MA, 3rd edition, 2005.
- [Com18] Patrick L Combettes. Perspective functions: Properties, constructions, and examples. *Set-Valued and Variational Analysis*, 26(2):247–264, 2018.
- [DDB20] Anthony Downward, Oscar Dowson, and Regan Baucke. Stochastic dual dynamic programming with stagewise-dependent objective uncertainty. *Operations Research Letters*, 48(1):33–39, 2020.
- [GSC19] Vincent Guigues, Alexander Shapiro, and Yi Cheng. Duality and sensitivity analysis of multistage linear stochastic programs. *arXiv preprint arXiv:1911.07080*, 2019.
- [GZ13] Horand Gassmann and William T Ziemba. *Stochastic Programming: applications in finance, energy, planning and logistics*, volume 4. World Scientific, 2013.
- [LCC⁺20] Vincent Leclère, Pierre Carpentier, Jean-Philippe Chancelier, Arnaud Lenoir, and François Pacaud. Exact converging bounds for stochastic dual dynamic programming via fenchel duality. *SIAM Journal on Optimization*, 30(2):1223–1250, 2020.
- [PdMF13] Andrew Philpott, Vitor de Matos, and Erlon Finardi. On solving multistage stochastic programs with coherent risk measures. *Operations Research*, 61(4):957–970, 2013.
- [PP91] Mario VF Pereira and Leontina MVG Pinto. Multi-stage stochastic optimization applied to energy planning. *Mathematical programming*, 52(1-3):359–375, 1991.
- [RBHdM19] Hamed Rahimian, Güzin Bayraksan, and Tito Homem-de Mello. Identifying effective scenarios in distributionally robust stochastic programs with total variation distance. *Mathematical Programming*, 173(1):393–430, 2019.
- [Rus10] Andrzej Ruszczyński. Risk-averse dynamic programming for markov decision processes. *Mathematical programming*, 125(2):235–261, 2010.
- [SDR09] Alexander Shapiro, Darinka Dentcheva, and Andrzej Ruszczyński. *Lectures on stochastic programming: modeling and theory*. SIAM, 2009.

- [Sha12] Alexander Shapiro. Minimax and risk averse multistage stochastic programming. *European Journal of Operational Research*, 219(3):719–726, 2012.
- [STdCS13] Alexander Shapiro, Wajdi Tekaya, Joari Paulo da Costa, and Murilo P Soares. Risk neutral and risk averse stochastic dual dynamic programming method. *European Journal of Operational Research*, 224(2):375–391, 2013.
- [ZAS19] Jikai Zou, Shabbir Ahmed, and Xu Andy Sun. Stochastic dual dynamic integer programming. *Mathematical Programming*, 175(1):461–502, 2019.

A Dual SDDP algorithm

Algorithm 2 presents the details of the dual dynamic programming algorithm used to solve the regularized dual problem in the recursion (13), which we recall here for ease of reference:

$$D_T(\pi_T, \gamma_T) = -\bar{x}_T^\top \max(\pi_T, 0) \quad (19a)$$

$$D_t(\pi_t, \gamma_t) = \sup_{\zeta, \gamma_j, \lambda_j, \pi_j, \xi_j} -\bar{x}_t^\top \zeta + \sum_{j \in [J]} -d_j^\top \lambda_j - \bar{y}_{t+1}^\top \xi_j + D_{t+1}(\pi_j, \gamma_j) \quad (19b)$$

$$\text{s.t. } \gamma \in \gamma_t \mathcal{Q} \quad (19c)$$

$$\zeta + \sum_j B_j^\top \lambda_j \geq \pi_t \quad (19d)$$

$$\pi_j + A_j^\top \lambda_j = 0 \quad \forall j \in [J_t] \quad (19e)$$

$$\gamma_j c_j + T_j^\top \lambda_j + \xi_j \geq 0 \quad \forall j \in [J_t] \quad (19f)$$

$$|\pi_j| \leq \gamma_j L_{t+1} \quad \forall j \in [J_t] \quad (19g)$$

$$\zeta \geq 0, \xi_j \geq 0. \quad (19h)$$

where the recursion defined by equations (19b)–(19h) applies for all $t \in \{0, 1, \dots, T-1\}$.

Recall that \bar{x}_t and \bar{y}_{t+1} are upper bounds on the norm of the state and control variables, and L_{t+1} is a Lipschitz constant on the primal value function V_t . Note that ζ and ξ_j can be interpreted as slack variables in the dual with exact penalization given by the bounds on the

primal variables.

Algorithm 2: Dual SDDP algorithm, for risk-averse problems

Data: Valid upper bounds \mathfrak{D}_t^0 for the dual functions D_t
Data: Lipschitz constants L_t bounding the dual states π_t
Parameter: Number of iterations N
Parameter: Tolerance tol for small probabilities
Parameter: Smoothing constant ε for scenario sampling
Result: Upper bound for problem (1)
Result: Improved upper bounds \mathfrak{D}_t^N for the dual functions D_t

```

1 Set UpperBound  $\leftarrow +\infty$ 
2 for  $k = 0$  to  $N$  do
    // Compute initial state and update upper bound
3   Solve  $\sup_{\pi_0} \pi_0^\top x_0 + \mathfrak{D}_0^k(\pi_0, 1)$ , save the optimal value  $d$ , optimal state  $\pi_0$  and set
       $\gamma_0 \leftarrow 1$ 
4   Set UpperBound  $\leftarrow d$ 
5   if  $k == N$  then return UpperBound,  $\mathfrak{D}_t^N$ 
    // Forward Pass
6   for  $t = 0$  to  $T - 1$  do
7     Solve the optimization problem:
        
$$\begin{aligned}
 D_t(\pi_t, \gamma_t) = \sup_{\zeta, \gamma_j, \lambda_j, \pi_j, \xi_j} & -\bar{x}_t^\top \zeta + \sum_{j \in [J_t]} (-d_j^\top \lambda_j - \bar{y}_{t+1}^\top \xi_j + \mathfrak{D}_{t+1}^k(\pi_j, \gamma_j)) \\
 \text{s.t.} & \gamma \in \gamma_t \mathcal{Q} \\
 & \zeta + \sum_j B_j^\top \lambda_j \geq \pi_t \\
 & \pi_j + A_j^\top \lambda_j = 0 & \forall j \in [J_t] \\
 & \gamma_j c_j + T_j^\top \lambda_j + \xi_j \geq 0 & \forall j \in [J_t] \\
 & |\pi_j| \leq \gamma_j L_{t+1} & \forall j \in [J_t] \\
 & \zeta \geq 0, \xi_j \geq 0
 \end{aligned}$$


(*)


        save the optimal variables  $\pi_j$ ,  $\gamma_j$ , and the optimal value  $v_t$ 
        // Construct a valid cut and add it to  $\mathfrak{D}_t$ 
8     Set  $x_t \leftarrow$  the dual multiplier of the constraint  $\zeta + \sum_j B_j^\top \lambda_j \geq \pi_t$ 
9     Set  $z_t \leftarrow$  the dual multiplier for  $\gamma \in \gamma_t \mathcal{Q}$ 
        // Sanity check
10    if  $v_t \not\approx x_t^\top \pi_t + z_t \cdot \gamma_t$  then Warn numerical instability
11    Let  $C(\pi, \gamma) := x_t^\top \pi + z_t \cdot \gamma$ 
12    Set  $\mathfrak{D}_t^{k+1} \leftarrow \min(\mathfrak{D}_t^k, C)$ 
        // Prepare for next stage
13    Choose the next branch  $\hat{j}$  among all  $J_t$  branches with probability proportional to
       $\gamma_j + \varepsilon$ 
14    if  $\hat{j} > tol$  then // Normalize state
      | Set  $\pi_{t+1} \leftarrow \pi_{\hat{j}}/\gamma_{\hat{j}}$ , and  $\gamma_{t+1} \leftarrow 1$ 
15    else // Round down
16    | Set  $\pi_{t+1} \leftarrow \pi_{\hat{j}}$ , and  $\gamma_{t+1} \leftarrow 0$ 
17

```

The dual algorithm is initialized with upper-approximations \mathfrak{D}_t^0 of the dual value functions D_t , which must be guaranteed upper bounds. One possibility is to compute them from the costs c_t and the bounds \bar{y}_t of the control variables of the primal problem, since the stage costs are at most $\max_{0 \leq \mathbf{y}_t \leq \bar{\mathbf{y}}_t} \mathbf{c}_t^\top \mathbf{y}_t$. Another possibility consists in doing a backward pass, as described in Remark 6 below, on any admissible dual trajectory (e.g. $(\pi_t = 0, \gamma_t = 1)$ for all t).

Line 3 of Algorithm 2 computes an initial dual state π_0 given the current approximation \mathfrak{D}_0^k . Indeed, from proposition 5, we know that the primal problem has optimal value

$$\sup_{\pi_0} \pi_0^\top x_0 + D_0(\pi_0, 1), \quad (20)$$

where x_0 is the primal initial state. This dual state can (and often does) change between iterations.

From this initial state, Problem (*) in line 7 is analogous to equation (19b), with \mathfrak{D}_{t+1}^k in place of D_{t+1} . In an LP implementation, $\mathfrak{D}_{t+1}^k(\pi_j, \gamma_j)$ can be represented through a hypographical variable z_j for each scenario j , and cuts C for \mathfrak{D}_{t+1} become linear constraints of the form

$$z_j \leq C^\kappa(\pi_j, \gamma_j), \quad \kappa \in [k]. \quad (21)$$

Solving Problem (*) yields solutions $(\pi_j, \gamma_j)_{j \in [J]}$ corresponding to the outgoing states for all realizations of ξ_{t+1} .

Line 13 randomly selects the next state, in a way that each branch has a positive probability to be chosen, with a preference towards the scenarios which most contribute to the value function. More precisely, the probability of choosing a branch j is proportional to $\gamma_j + \epsilon$, where ϵ is a small positive number and γ the current change-of-measure. Note that for some risk measures, like the AV@R (but not strict combinations of AV@R and Expectation), the current change of measure could attribute 0 probability to some realizations, preventing exploration, and thus convergence of the dynamic programming algorithm.

By homogeneity of the value functions, the probabilities γ_t are normalized in line 15 at each stage, and π_t is normalized accordingly. We have observed that this usually improves the numerical stability of the algorithm. Indeed, the value of γ_t is the (current) risk-adjusted probability of the stage- t scenario, which decreases as t increases. Since most solvers have both a relative and an absolute tolerance, the homogeneity of the stage problems with respect to (π_t, γ_t) might result in a very large relative error of the algorithm when γ_t becomes too small. Finally, in line 17, the probabilities γ_t are rounded down to 0 if they are too small.

After performing N iterations, the algorithm stops, returning the current best upper bound for Problem 1, and the current piecewise linear approximations \mathfrak{D}_t^N of the dual functions D_t .

Remark 6 (Backward pass). In the primal SDDP algorithm (risk-averse or not), the stage problem can be decomposed in J_t subproblems, one for each realization of ξ_{t+1} . In particular, the optimal next-state for realization $j \in [J_t]$ is given by solving a problem independent of other possible realizations of ξ_{t+1} . However, computing a cut requires solving a problem that depends on all realizations of ξ_{t+1} . Thus, standard implementations of primal SDDP have a forward phase, to determine trajectories, and a backward phase, to compute cuts; the latter is slower, solving $[J_t]$ more problems at stage t .

In the dual formulation, this decomposition is no longer possible due to the coupling constraints (19c) and (19d). In particular, to determine the optimal next-state value for a given realization $j \in [J_t]$, one needs to solve a problem that depends on all realizations of ξ_{t+1} . Thus, computing a dual trajectory also provides all the information needed to compute a cut. This is why Algorithm 2 only has a forward phase.

Naturally, it is also possible to add cuts in a backward fashion, which would need then to solve a problem similar to equation (*), but with an extra cut, using \mathfrak{D}_{t+1}^{k+1} . This speeds up

the information flow back to the first stage, at the cost of (approximately) doubling the time per iteration. This might be especially useful in the first few iterations to replace the initial, user-given, upper bound.

B Detailed description of the numerical experiments

The numerical example we used comes from the Brazilian Hydrothermal Energy planning problem. In its long-term formulation, the reservoirs and hydro dams are aggregated into 4 subsystems, Southeast, South, Northeast and North. Each subsystem also corresponds to a region with an associated total energy demand. Long-distance transmission lines connect the South with the Southeast, Southeast with Northeast, and an extra interconnection node (modeled as a 5th subsystem), to the North, Northeast and Southeast subsystems. In each subsystem, the demand for energy in each month, $d_{s,t}$, is supposed to be known; the demand of subsystem 5 is zero. Not satisfying this demand with thermal or hydro-generation and exchanges with another subsystem, leads to energy curtailment, as described in (22b).

For simplicity, this model considers energy equivalents for water volumes, so the stored volumes are represented by $x_{s,t}$, the equivalent energy in the reservoir of subsystem s at the end of stage t (and the beginning of stage $t + 1$). For system s , the hydro generation during stage t is given by $h_{s,t}$, the (equivalent energy) inflow by $\text{inflow}_{s,t}$, and (equivalent energy) spillage by $\text{spill}_{s,t}$, resulting in the dynamic equation (22c). Constraints (22d) to (22g) represent physical bounds on hydro storage, hydro production, thermal production and exchanges. The spillage is akin to a slack variable, and therefore positive as enforced by (22h). Remaining constraints define four ranges for energy curtailment.

Thermal power plants are represented individually, each with its own minimum and maximum generation limits, \underline{g}_j , \bar{g}_j , as well as costs per MWh c_j . Each thermal plant is located in a given subsystem s , and the set T_s collects the indices j of thermal plants in subsystem s . If demand is not met, curtailment has increasing costs CD_k for $k = \{1, 2, 3, 4\}$, corresponding to curtailment below 5%, 10%, 20% or 100% of the demand $d_{s,t}$ of the subsystem.

Therefore, the (primal) dynamic programming recursion becomes:

$$V_t(x_{t-1}) = \min \rho \left[\sum_j c_j g_{j,t} + \sum_k \sum_s CD_k cur_{s,k,t} + \text{spill_pen} \sum_s \text{spill}_{s,t} + \sum_{s,s'} \text{xch_pen}_{s,s'} ex_{s,s',t} + V_{t+1}(x_t) \right] \quad (22a)$$

$$\text{s.t. } d_{s,t} = h_{s,t} + \sum_{j \in T_s} g_{j,t} + \sum_k cur_{s,k,t} + \sum_{s'} ex_{s',s,t} - ex_{s,s',t}, \quad \forall t, \forall s \quad (22b)$$

$$x_{s,t} = x_{s,t-1} + \text{inflow}_{s,t} - h_{s,t} - \text{spill}_{s,t} \quad \forall t, \forall s \quad (22c)$$

$$0 \leq x_{s,t} \leq \bar{x}_s \quad \forall t, \forall s \quad (22d)$$

$$0 \leq h_{s,t} \leq \bar{h}_s \quad \forall t, \forall s \quad (22e)$$

$$\underline{g}_j \leq g_{j,t} \leq \bar{g}_j \quad \forall t, \forall j \quad (22f)$$

$$0 \leq ex_{s,s',t} \leq \bar{ex}_{s,s'} \quad \forall t, \forall s, \forall s' \quad (22g)$$

$$0 \leq \text{spill}_{s,t} \quad \forall t, \forall s \quad (22h)$$

$$0 \leq cur_{s,1,t} \leq 5\% \cdot d_{s,t} \quad \forall t, \forall s \quad (22i)$$

$$0 \leq cur_{s,2,t} \leq 5\% \cdot d_{s,t} \quad \forall t, \forall s \quad (22j)$$

$$0 \leq cur_{s,3,t} \leq 10\% \cdot d_{s,t} \quad \forall t, \forall s \quad (22k)$$

$$0 \leq cur_{s,4,t} \leq 80\% \cdot d_{s,t} \quad \forall t, \forall s. \quad (22l)$$

The stage costs include thermal generation costs, and curtailment costs for every level and subsystem. Moreover, it includes penalties for both energy spillage and exchange.

The problem instances we solve consider uncertainties on the inflows only. We take the historical inflows for each month as scenarios, which are then sampled independently along the planning horizon. This amounts to 82 realizations per stage, corresponding to the years 1931–2012, inclusive.

Data, such as variable bounds and unit costs for the example we deal with can be found at the supplementary file `data.jl`. A further supplementary file `demand.jl` contains the series of demands, for each subsystem, along the stages. The historical series of inflows we use can be found in the last supplementary file, `eafs.npz`.

A complete setup, parsing the data and building the corresponding matrices for the dual recursion can be found at https://github.com/bfpc/DualSDDP.jl/blob/91a50a9c9eb16db6acc4a046e4471c9737cd01a1/examples/4d_hydro/.

C Impact of Lipschitz estimate on convergence

We performed two experiments to assess the impact of providing a larger Lipschitz constant than the true one. In order to do so, we used algorithm 2 with a tight Lipschitz constant, then a 10 times larger one, and finally a 100 times larger one. We assessed different combinations of risk-aversion, and compared the evolution of the upper bounds to the best lower bound found with the primal SDDP.

The first graph, in Figure 2, corresponds to a simplified hydrothermal problem, given by the same recursion (22), but with only three thermal units, two reservoirs, and one interconnection between the two corresponding subsystems. We notice that the initial estimates are larger for larger Lipschitz estimates, but after some iterations the impact of a worse Lipschitz estimate is negligible.

The second one, in Figure 3, corresponds to the larger 4-reservoir setting of the previous section. There, we remark a much lower sensitivity of the bounds with respect to the candidate Lipschitz constant. For example, the gaps at the 100th iteration in the case of $\alpha = 0.3$ and $\beta = 0.5$ are, respectively, 14.95, 14.72 and 14.72 for factors 1, 10 and 100, which is such a small difference that it is not visible in the figure.

For completeness, we report the relative gaps, in %, for both experiments in Table 2, for several intermediate iterations.

(α, β)	Factor	2 reservoir Iteration					4 reservoir Iteration			
		1	10	20	50	100	10	100	200	300
(0.10, 0.10)	1	590.4	448.6	16.32	0.42	0.19	304.04	3.66	1.94	1.61
	10	1129.1	538.4	20.58	0.37	0.21	304.04	3.66	1.94	1.61
	100	6515.6	659.4	20.58	0.37	0.21	304.04	3.66	1.94	1.61
(0.10, 0.50)	1	1097.4	817.5	47.49	6.58	1.58	542.00	10.23	4.86	3.30
	10	2031.6	1000.5	42.94	5.73	1.84	542.00	10.23	4.86	3.30
	100	11373.8	1138.4	42.94	5.73	1.84	542.00	10.23	4.86	3.30
(0.10, 0.90)	1	2643.2	1462.4	187.70	20.90	7.53	1436.20	26.41	14.24	10.31
	10	4783.5	1757.4	168.36	21.39	6.73	1436.20	26.45	14.37	10.33
	100	26186.4	1757.4	168.36	21.39	6.73	1436.20	26.45	14.42	10.66
(0.30, 0.10)	1	794.4	596.9	23.97	1.25	0.65	383.48	5.16	2.42	1.88
	10	1492.3	722.2	26.51	1.16	0.69	383.48	5.16	2.42	1.88
	100	8470.8	828.2	26.51	1.16	0.69	383.48	5.16	2.42	1.88
(0.30, 0.50)	1	1385.2	721.1	61.54	7.44	2.21	687.45	14.95	5.90	3.85
	10	2544.0	765.4	94.13	8.12	2.54	687.45	14.72	5.64	3.83
	100	14131.6	911.3	60.85	8.74	2.11	687.45	14.72	5.64	3.83
(0.30, 0.90)	1	2833.4	1771.2	283.57	24.23	7.30	1505.73	28.37	14.88	10.06
	10	5122.1	1954.3	202.89	22.78	8.02	1505.73	28.37	14.88	10.06
	100	28009.1	1943.0	210.18	27.93	7.25	1505.73	28.37	14.88	10.06
(0.50, 0.10)	1	1032.7	768.6	39.17	1.46	0.57	574.96	6.06	2.46	1.72
	10	1916.5	938.9	41.30	1.55	0.57	574.96	5.50	2.67	1.75
	100	10754.4	1046.1	43.92	1.65	0.59	574.96	6.67	2.74	1.72
(0.50, 0.50)	1	1695.5	1047.3	124.57	9.26	2.91	920.73	17.26	7.67	5.38
	10	3096.3	1040.5	92.07	11.03	2.92	920.73	17.26	7.67	5.38
	100	17104.7	1040.5	92.07	11.03	2.92	920.73	17.26	7.67	5.45
(0.50, 0.90)	1	2976.4	1846.5	210.09	24.36	8.41	1659.86	31.14	15.66	10.35
	10	5376.6	1945.9	196.51	27.87	7.61	1659.86	31.14	15.66	10.35
	100	29379.1	2039.5	241.80	25.54	7.31	1659.86	31.14	15.66	10.35

Table 2: Relative gaps (%) for the 2-reservoir and 4-reservoir problems, for different factors corresponding to overestimating the Lipschitz constant.

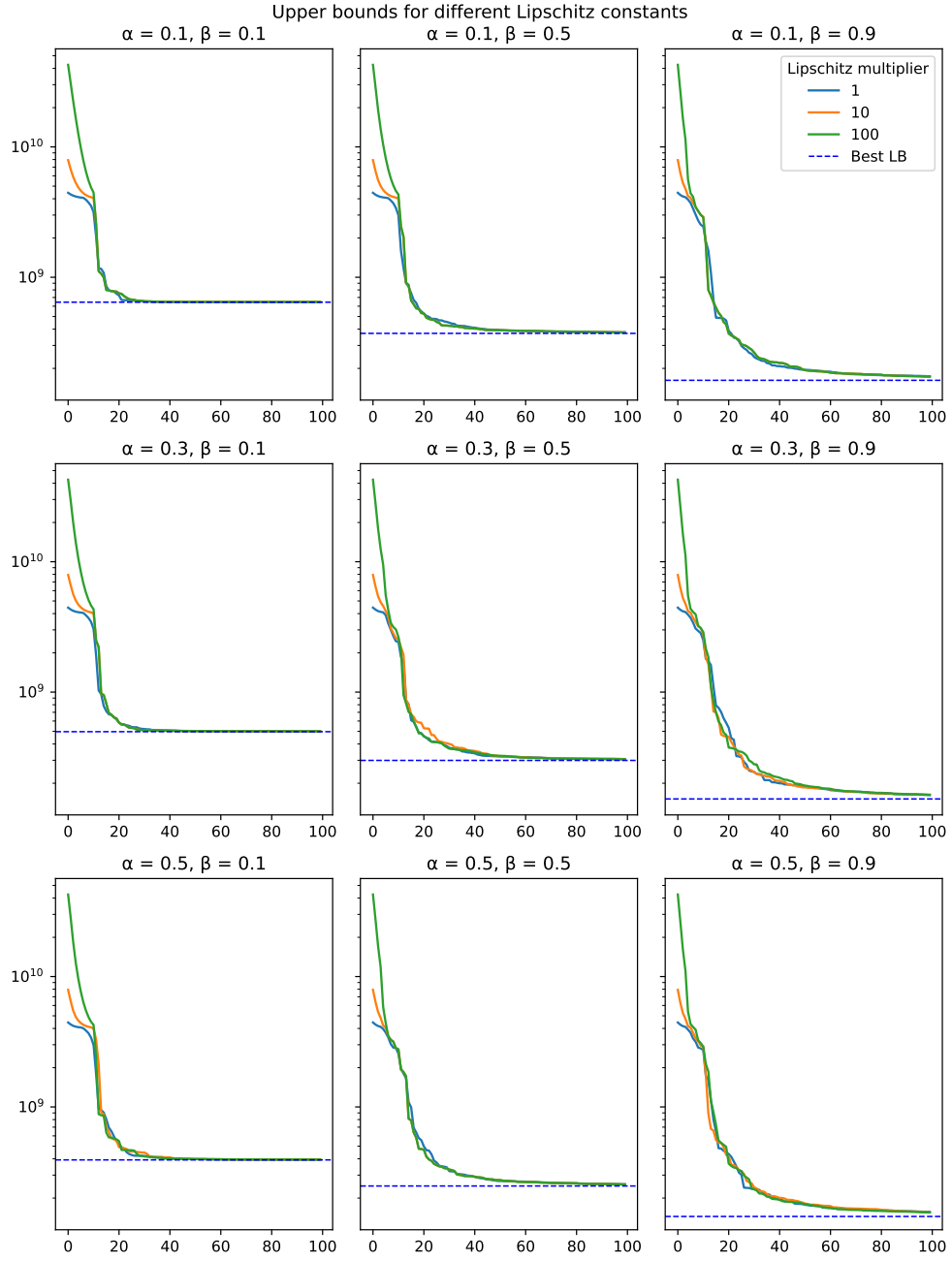


Figure 2: Upper bounds on the small 2-reservoir problem.

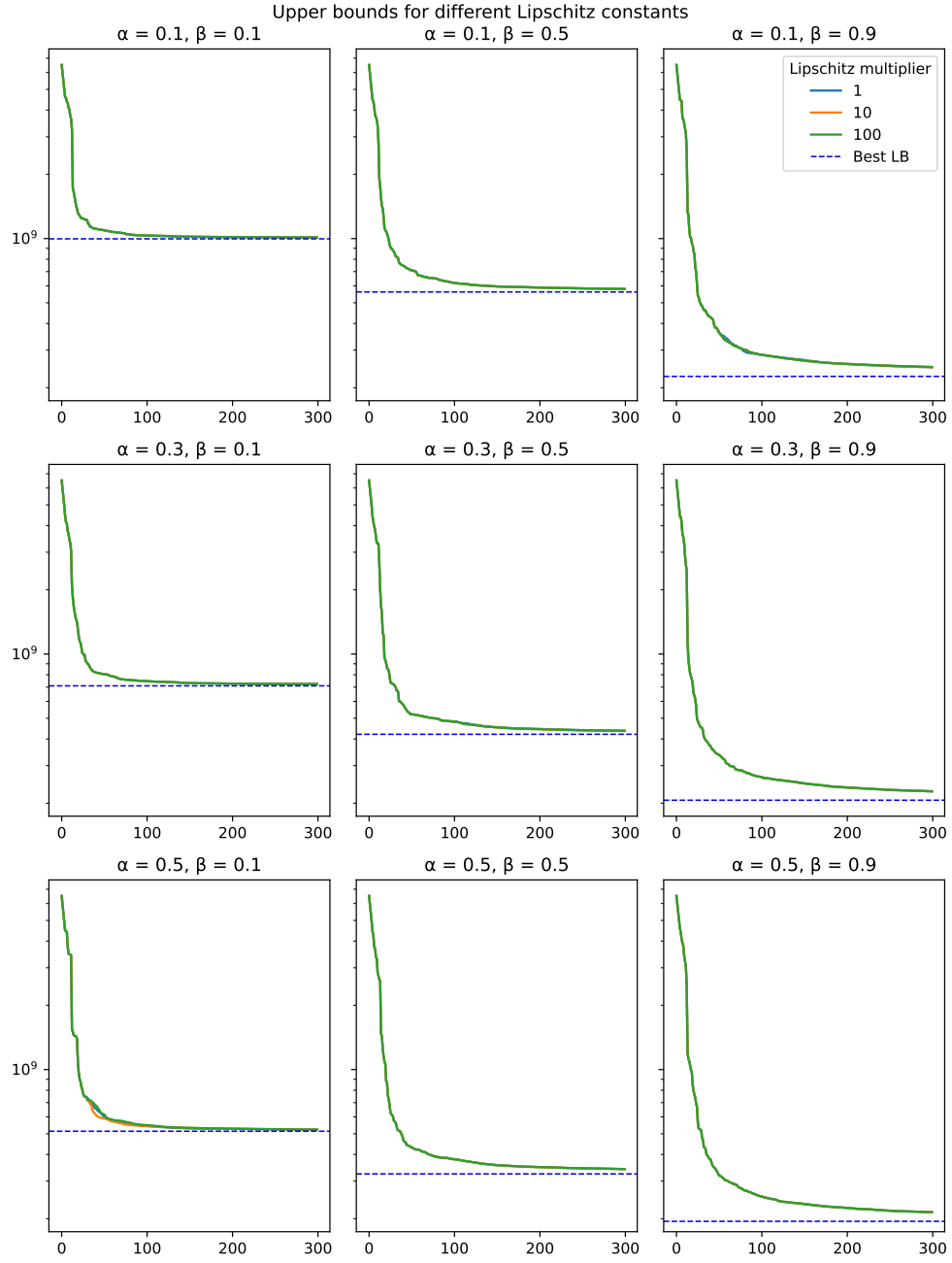


Figure 3: Upper bounds on the 4-reservoir problem.